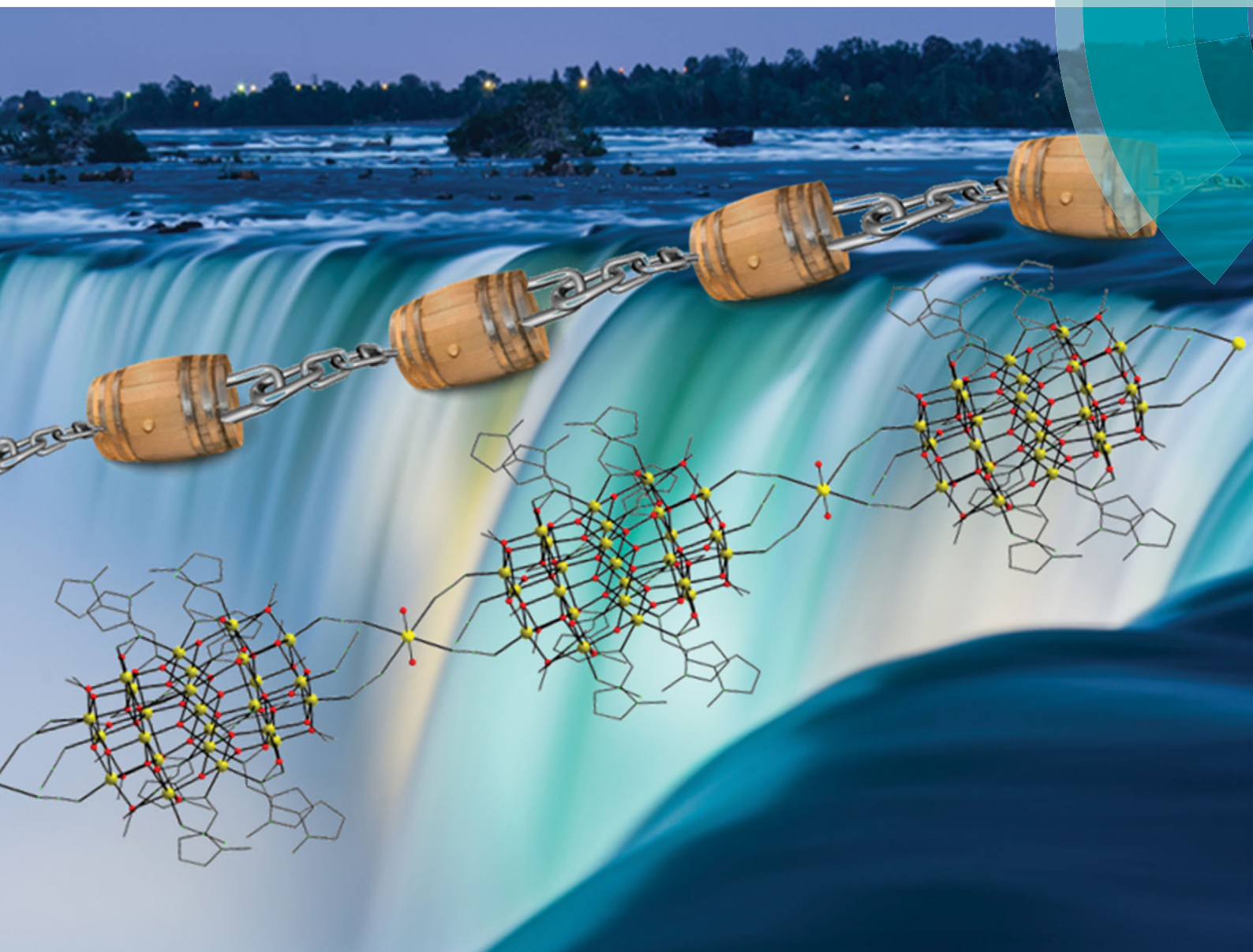


# ChemComm

Chemical Communications

[www.rsc.org/chemcomm](http://www.rsc.org/chemcomm)



ISSN 1359-7345



ROYAL SOCIETY  
OF CHEMISTRY

**COMMUNICATION**

Theocharis C. Stamatatos *et al.*  
Supramolecular chains of high nuclearity  $\{Mn^{III}_{25}\}$  barrel-like single molecule magnets

# Supramolecular chains of high nuclearity $\{\text{Mn}^{\text{III}}_{25}\}$ barrel-like single molecule magnets†

Cite this: *Chem. Commun.*, 2014, 50, 779

Received 16th September 2013,  
Accepted 30th October 2013

DOI: 10.1039/c3cc47094f

www.rsc.org/chemcomm

Dimosthenis P. Giannopoulos,<sup>a</sup> Annaliese Thuijs,<sup>b</sup> Wolfgang Wernsdorfer,<sup>c</sup> Melanie Pilkington,<sup>a</sup> George Christou<sup>b</sup> and Theocharis C. Stamatatos\*<sup>a</sup>

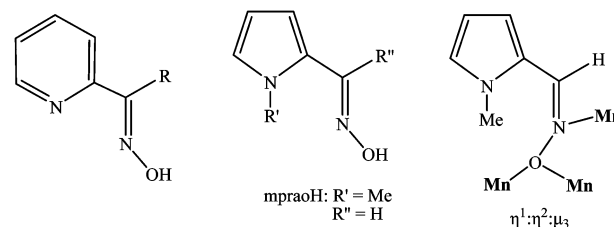
**The first application of 1-methyl-1H-pyrrole-2-carbaldehyde oxime as a ligand for the coordination of paramagnetic transition metal ions has afforded a new  $\{\text{Mn}^{\text{III}}_{25}\}$  barrel-like cluster linked via  $\text{Na}^+$  cations into a 1D polymeric topology that exhibits single-molecule magnetic behaviour.**

The field of single-molecule magnets (SMMs) has grown considerably over the past two decades to include families of transition metal complexes incorporating paramagnetic ions with moderate-to-high oxidation states,<sup>1</sup> as well as complexes assembled from trivalent lanthanide<sup>2</sup> and actinide<sup>3</sup> metal ions. Research efforts in this field have been largely driven by the two requirements for molecules to exhibit SMM behaviour namely, a bistable electronic ground state arising from an often large, ground state spin value ( $S$ ), coupled with magnetic anisotropy, attributed to a negative zero-field splitting ( $zfs$ ) parameter ( $D$ ).<sup>4</sup> Such a combination affords an energy barrier ( $|D|S^2$ ) for reversal of the magnetization. Thus, at sufficiently low temperatures, these molecules function as nanoscale magnetic particles and straddle the classical/quantum interface by displaying not just classical magnetization hysteresis, but also quantum tunneling of magnetization (QTM) and quantum phase interference.<sup>5</sup>

In this context, SMMs have been proposed as promising candidates for potential applications in information storage and spintronics at the molecular level and for use as quantum bits in quantum computation.<sup>6</sup> For SMMs to be incorporated into devices the molecules must be coupled to each other, and strategies to weakly couple SMMs while preserving their bistability are being actively pursued.<sup>7</sup> Furthermore, in order for the magnetic properties of SMMs to be commercially viable, improvements in both

their blocking temperatures and coercive fields are necessary. Strategies that enable the rational modification of the bridging units between SMMs represent a promising approach for maximizing these parameters.<sup>8,9</sup> The self-assembly of SMMs into multi-dimensional architectures therefore remains a challenge for coordination chemists working at the interface of supramolecular chemistry and molecular magnetism.<sup>10</sup>

With respect to the preparation of novel families of SMMs, we and others have had success in developing high nuclearity 3d metal clusters based on 2-pyridyloxime ligands, (py)C(R)NOH ( $R = \text{various}$ ; Scheme 1, left).<sup>7,11</sup> More recently we have shown that the related 2-pyrrolyloximes (Scheme 1, middle) also act as bridging ligands for the coordination of paramagnetic metal centers. The simplest ligand initially chosen was pyrrole-2-carboxaldehyde oxime (praoH<sub>2</sub>;  $R' = R'' = \text{H}$ ; Scheme 1, middle) which forms a family of Fe<sub>3</sub>, Fe<sub>6</sub>, Fe<sub>10</sub> and Fe<sub>12</sub> clusters, all with very small or zero  $S$  values.<sup>12</sup> However, attempts to generate similar Mn<sup>III</sup> complexes, which may offer large magnetic anisotropy, were thwarted by the presence of the pyrrole N-H functionality, a well-known reducing group. In order to inhibit such redox activity, we have turned our attention to the closely related ligand, 1-methyl-1H-pyrrole-2-carbaldehyde oxime (mpraoH;  $R' = \text{Me}$ ,  $R'' = \text{H}$ ; Scheme 1, middle). Here we show that the alkylated mpraoH ligand is robust with respect to redox activity and supports the formation of high nuclearity clusters. The title compound behaves as an SMM, and the diamagnetic



**Scheme 1** The two families of 2-pyridyloxime (left) and 2-pyrrolyloxime (middle) ligands discussed in the text, and the crystallographically established coordination mode of mprao<sup>-</sup> in complex **1** (right).

<sup>a</sup> Department of Chemistry, Brock University, St. Catharines, Ontario, L2S 3A1, Canada. E-mail: tstatatos@brocku.ca; Tel: +1-905-688-5550 Ext. 3400

<sup>b</sup> Department of Chemistry, University of Florida, Gainesville, Florida 32611-7200, USA

<sup>c</sup> Institut Néel, CNRS, Nanoscience Department, BP 166, 380412 Grenoble Cedex 9, France

† Electronic supplementary information (ESI) available: Crystallographic data (CIF format), synthetic details, and various structural and magnetism figures of **1**. CCDC 950209. For ESI and crystallographic data in CIF or other electronic format see DOI: 10.1039/c3cc47094f

$\text{Na}^+$  coordinated ions help organize the individual quantum spins on the SMMs into supramolecular chains.

Reaction of  $\text{mpraoH}$  with  $\text{Mn}(\text{ClO}_4)_2 \cdot 6\text{H}_2\text{O}$ ,  $\text{NEt}_3$  and  $\text{NaN}_3$  in a 1:1:1:1 molar ratio in  $\text{MeCN}-\text{MeOH}$  (2:1 v/v) in air afforded a dark brown solution indicative of the presence of  $\text{Mn}^{\text{III}}$  and/or  $\text{Mn}^{\text{IV}}$  ions. Layering this solution with  $\text{Et}_2\text{O}$  afforded, after four days, X-ray quality, dark brown plate-like crystals of the 1D coordination polymer  $[\text{Mn}_{25}\text{NaO}_{20}(\text{OME})_{12}(\text{N}_3)_{12}(\text{mprao})_{12}(\text{H}_2\text{O})_2]_n \cdot 8n\text{MeOH} (\mathbf{1} \cdot 8\text{MeOH})_n$  in 30% yield. $\ddagger$

Compound **1** crystallizes in the triclinic space group  $P\bar{1}$  with the molecule possessing crystallographic  $C_i$  symmetry. The core of the cluster is held together by twelve  $\mu_4\text{-O}^{2-}$ , eight  $\mu_3\text{-O}^{2-}$ , six  $\mu_3$ - and six  $\mu\text{-OME}^-$  ions, as well as the deprotonated oximate arms of twelve  $\eta^1:\eta^2:\mu_3$   $\text{mprao}^-$  groups (Fig. 1, top). The  $\text{Mn}_{25}$  core can be dissected into five parallel layers of three types with an ABCBA arrangement (Fig. 1, bottom). Layer A is a  $\text{Mn}^{\text{III}}_3$  triangular unit with a capping  $\mu_3\text{-O}^{2-}$  ion; layer B is a  $\text{Mn}^{\text{III}}_6$  triangle that can be described as three corner-fused  $\text{Mn}^{\text{III}}_3$  triangular moieties each capped by a  $\mu_3\text{-O}^{2-}$  ion; and layer C is a disk-like  $\text{Mn}^{\text{III}}_7$  unit, reminiscent of the known Anderson-type structure. Each layer is held together and linked to its neighbours by a combination of oxido, methoxido, and/or oximate bridges. Whilst the core geometry is similar to that previously observed for the mixed-valence  $\text{Mn}^{\text{II}}_6\text{Mn}^{\text{III}}_{18}\text{Mn}^{\text{IV}}$  barrels  $[\text{Mn}_{25}\text{O}_{18}(\text{OH})_2(\text{N}_3)_{12}(\text{pdm})_6(\text{pdmH})_6]^{2+}$  and  $[\text{Mn}_{25}\text{O}_{18}(\text{OH})(\text{OME})(\text{hmp})_6(\text{pdm})_6(\text{pdmH})_6]^{8+}$  ( $\text{pdmH}_2 = 2,6\text{-pyridinedimethanol}$ ;  $\text{hmpH} = 2\text{-(hydroxymethyl)pyridine}$ ), $^{13}$  the oxidation states of the Mn ions in **1** are all assigned to  $\text{Mn}^{\text{III}}$ . The oxidation states were determined qualitatively by inspection of metric parameters and detection of  $\text{Mn}^{\text{III}}$  Jahn–Teller (JT) elongation axes for all crystallographically independent Mn ions, as well as quantitatively by bond valence sum (BVS) $^{14}$  calculations (Table S1, ESI $\dagger$ ). In the case of the central  $\text{Mn}^{\text{III}}$  atom ( $\text{Mn}_6$ ), which lies on a

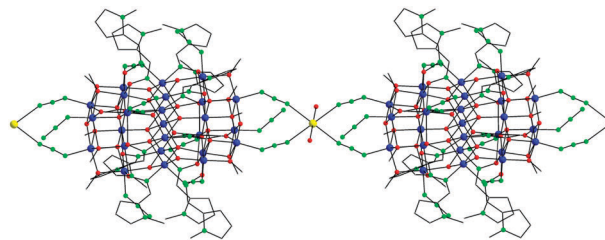


Fig. 2 A small portion of the 1D polymeric structure of **1**. Colour scheme as in Fig. 1; Na yellow. H-atoms are omitted for clarity.

crystallographic inversion centre, both the intermediate for a  $\text{Mn}^{\text{II}}/\text{Mn}^{\text{III}}$  ion BVS value and the absence of a clear JT axis are assigned to the static disorder among the three symmetry-equivalent  $\text{O}(15,19,22)\text{-Mn}(6)\text{-O}(15',19',22')$  axes. $^{15}$

Peripheral ligation about the  $\text{Mn}_{25}$  core is provided by twelve terminally bound  $\text{N}_3^-$  ions, four of which assemble end-to-end linking the  $\text{Mn}_{25}$  units to a  $\text{Na}^+$  ion at each end, affording a 1D linear chain (Fig. 2). The coordination sphere of the octahedral  $\text{Na}^+$  cations is completed by two axially bonded  $\text{H}_2\text{O}$  molecules. The shortest  $\text{Mn}\cdots\text{Mn}$  separation between the  $\text{Mn}_{25}$  magnetic units is appreciably large (11.23(5) Å), while there are no other significant intermolecular interactions between the 1D chains. The overall barrel shape and nanometer size of the  $\text{Mn}_{25}$  unit in **1** are emphasized in the space-filling plots shown in Fig. S1 and S2 (ESI $\dagger$ ); the cluster has a length of  $\sim 18.5$  Å and a diameter of  $\sim 17.2$  Å, excluding the H-atoms.

Solid-state, dc magnetic susceptibility ( $\chi_M$ ) data for an air-dried sample of **1** were collected in the temperature range 5–300 K and in an applied field of 0.1 T. The data reveal that  $\chi_M T$  steadily decreases from  $73.48 \text{ cm}^3 \text{ K mol}^{-1}$  at 300 K to  $20.62 \text{ cm}^3 \text{ K mol}^{-1}$  at 5.0 K (Fig. S3, ESI $\dagger$ ). The 300 K value is slightly less than the spin-only ( $g = 2$ ) value of  $75 \text{ cm}^3 \text{ K mol}^{-1}$  for 25  $\text{Mn}^{\text{III}}$  non-interacting ions, indicating the presence of dominant anti-ferromagnetic exchange interactions within the cage. The 5 K value suggests that **1** possesses a fairly large ground state spin value of possibly  $S = 6$ ; the spin-only ( $g = 2$ ) value for  $S = 6$  is  $21 \text{ cm}^3 \text{ K mol}^{-1}$ . Given the size of the  $\text{Mn}_{25}$  molecule, and the resulting number of inequivalent exchange constants, it is not possible to determine the individual pairwise  $\text{Mn}_2$  exchange interaction parameters. Thus, we concentrated instead on characterizing the ground state spin,  $S$ , and the  $zfs$  parameter,  $D$ , by performing magnetization ( $M$ ) vs. dc field measurements in a magnetic field and temperature range 1–70 kG and 1.8–10.0 K, respectively. Unfortunately, we were unable to obtain an acceptable fit for the data collected over the whole field range. This is a common problem in many large Mn clusters due to the population of low-lying excited states even at ultra-low temperatures, especially if some have an  $S$  value greater than that of the ground state.

A powerful complement to dc studies for determining the ground state of a system, and also to study magnetization dynamics, is ac magnetic susceptibility measurements which preclude any complications arising due to the presence of a dc field. These were performed in a 3.5 G ac field oscillating at different frequencies. The in-phase susceptibility ( $\chi_M'$ ) is

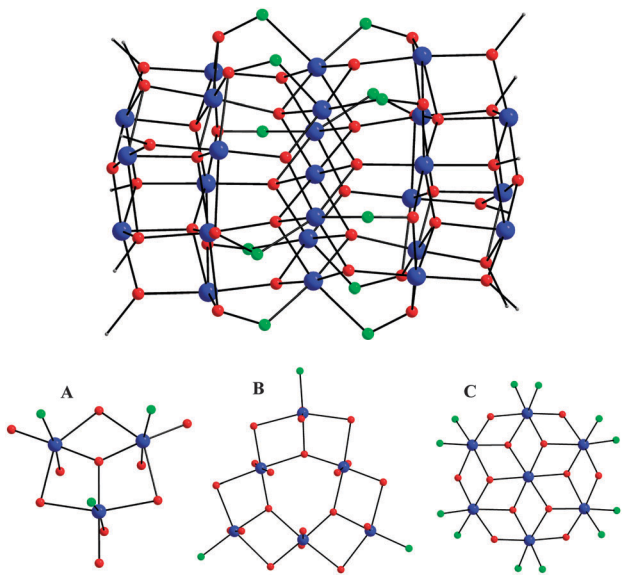


Fig. 1 (top) Core structure of the  $\{\text{Mn}^{\text{III}}_{25}\}$  barrel. (bottom) ORTEP representations of the three types of constituent  $\text{Mn}_x$  layers in **1**. Colour scheme:  $\text{Mn}^{\text{III}}$  blue; O red; N green; C grey.

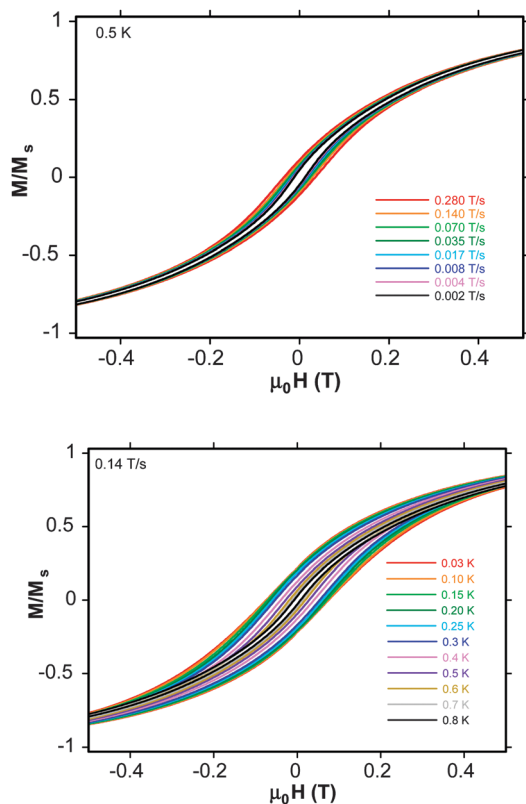


Fig. 3 Magnetization ( $M$ ) vs. applied dc field ( $H$ ) hysteresis loops for a single-crystal of **1**·8MeOH at the indicated field sweep rates (top) and temperatures (bottom). The magnetization is normalized to its saturation value ( $M_s$ ).

shown as  $\chi_M/T$  vs.  $T$  in Fig. S4 (ESI<sup>†</sup>) (top), and reveals several pertinent features: (i)  $\chi_M/T$  decreases linearly with decreasing temperature in the 4–15 K range, indicating depopulation of a high density of excited states with spin  $S$  greater than that of the ground state, which is in agreement with the conclusion of the dc studies; (ii) extrapolation of the  $\chi_M/T$  data from above  $\sim 4.0$  K to 0 K gives a value of  $\sim 21$  cm<sup>3</sup> K mol<sup>-1</sup>, which is indicative of an  $S = 6$  ground state with  $g = 2$ ; (iii) below  $\sim 4$  K, there is a frequency-dependent decrease in  $\chi_M/T$  and a concomitant appearance of frequency-dependent  $\chi_M''$  signals (Fig. S4, bottom, ESI<sup>†</sup>); such signals are an indication of the superparamagnetic-like slow relaxation of an SMM.

To confirm this last observation, magnetization vs. applied dc field data were collected on a single-crystal of **1**·8MeOH down at 0.03 K on a micro-SQUID. Hysteresis loops are seen below  $\sim 0.8$  K whose coercivities increase with increasing sweep rate (Fig. 3, top) and with decreasing temperature (Fig. 3, bottom), confirming **1** to be an SMM. These loops do not show the steps characteristic of quantum tunnelling, as expected for large SMMs which are more susceptible to various step-broadening effects.<sup>10,13,16</sup>

It should be noted that complex **1** is simply too complicated to rationalize the  $S = 6$  ground state on the basis of its structure alone. There are extensive spin frustration effects operating within the many fused Mn<sub>3</sub> triangular units, which render any spin assignment inaccurate and superficial.

In conclusion, we have established that the  $N$ -alkylation of a 2-pyrrolyloxime stabilizes the molecule with respect to oxidation. The resultant  $\text{mpao}^-$  ligand is therefore able to bridge Mn<sup>III</sup> centres affording a large polynuclear barrel-shaped {Mn<sup>III</sup><sub>25</sub>} cluster that is structurally related to the examples of mixed-valence Mn<sub>25</sub> barrel-like SMMs reported in the literature.<sup>13</sup> To date, this system represents the highest nuclearity Mn cluster which is organized into a 1D polymer through chelation with diamagnetic metal centers.<sup>17</sup> Given the apparent stability of these barrel-like clusters in multiple oxidation states, the redox activity of **1** is being actively pursued. Furthermore, strategies aimed at the selective replacement of the diamagnetic Na<sup>+</sup> cations with paramagnetic 4f-metal ions, targeting the rational assembly of **1** into new classes of SCMs, are currently under investigation.

This work was supported by Brock University and NSERC Discovery Grant (Th.C.S and M.P), CRC and CFI (M.P), the National Science Foundation (DMR-1213030 to G.C), the ERC Advanced Grant MolNanoSpin No. 226558 (WW).

## Notes and references

† Air-dried solid analyzed (C, H, N) as **1**. Calcd (found): C, 24.57 (24.68); H, 3.04 (3.33); N, 20.46 (20.34%). Crystal data for **1**: C<sub>92</sub>H<sub>156</sub>Mn<sub>25</sub>·NaN<sub>6</sub>O<sub>54</sub>,  $M_w = 4363.25$ , triclinic, space group  $P\bar{1}$  with  $a = 16.233(3)$  Å,  $b = 16.707(3)$  Å,  $c = 17.691(3)$  Å,  $\alpha = 63.270(6)^\circ$ ,  $\beta = 80.447(7)^\circ$ ,  $\gamma = 65.254(6)^\circ$ ,  $V = 3890.2(12)$  Å<sup>3</sup>,  $T = 150(2)$  K,  $Z = 1$ ,  $D_c = 1.862$  g cm<sup>-3</sup>, 54 391 reflections collected, 13 608 unique ( $R_{\text{int}} = 0.0659$ ),  $R_1 [I > 2\sigma(I)] = 0.0917$ ,  $wR_2 = 0.2206$  ( $F^2$ , all data).

- 1 G. Aromí and E. K. Brechin, *Struct. Bonding*, 2006, **122**, 1.
- 2 D. N. Woodruff, R. E. P. Winpenny and R. A. Layfield, *Chem. Rev.*, 2013, **113**, 5110.
- 3 J. D. Rinehart and J. R. Long, *J. Am. Chem. Soc.*, 2009, **131**, 12558.
- 4 D. Gatteschi and R. Sessoli, *Angew. Chem., Int. Ed.*, 2003, **42**, 268.
- 5 W. Wernsdorfer and R. Sessoli, *Science*, 1999, **284**, 133.
- 6 A. Candini, S. Klyatskaya, M. Ruben, W. Wernsdorfer and M. Affronte, *Nano Lett.*, 2011, **11**, 2634.
- 7 T. N. Nguyen, W. Wernsdorfer, K. A. Abboud and G. Christou, *J. Am. Chem. Soc.*, 2011, **133**, 20688.
- 8 W.-X. Zhang, R. Ishikawa, B. Breedlove and M. Yamashita, *RSC Adv.*, 2013, **3**, 3772.
- 9 D. Liu, Q. Zhou, Y. Chen, F. Yang, Y. Yu, Z. Shi and S. Feng, *Cryst. Growth Des.*, 2010, **10**, 2661 and references therein.
- 10 (a) E. E. Moushi, T. C. Stamatatos, W. Wernsdorfer, V. Nastopoulos, G. Christou and A. J. Tasiopoulos, *Angew. Chem., Int. Ed.*, 2006, **45**, 7722; (b) E. E. Moushi, T. C. Stamatatos, W. Wernsdorfer, V. Nastopoulos, G. Christou and A. J. Tasiopoulos, *Inorg. Chem.*, 2009, **48**, 5049 and references therein.
- 11 (a) C. J. Milios, T. C. Stamatatos and S. P. Perlepes, *Polyhedron*, 2006, **25**, 134; (b) C. Dendrinou-Samara, C. M. Zaleski, A. Evagorou, J. W. Kampf, V. L. Pecoraro and D. P. Kessissoglou, *Chem. Commun.*, 2003, 2668.
- 12 (a) A. B. Canaj, M. Siczek, A. P. Douvalis, T. Bakas, T. Lis and C. J. Milios, *Polyhedron*, 2013, **52**, 1411; (b) E. S. Koumoussi, A. Routzomani, T. N. Nguyen, D. P. Giannopoulos, C. P. Raptopoulou, V. Psycharis, G. Christou and T. C. Stamatatos, *Inorg. Chem.*, 2013, **52**, 1176.
- 13 (a) M. Murugesu, M. Habrych, W. Wernsdorfer, K. A. Abboud and G. Christou, *J. Am. Chem. Soc.*, 2004, **126**, 4766; (b) T. C. Stamatatos, K. A. Abboud, W. Wernsdorfer and G. Christou, *Angew. Chem., Int. Ed.*, 2007, **46**, 884.
- 14 W. Liu and H. H. Thorp, *Inorg. Chem.*, 1993, **32**, 4102.
- 15 (a) E. S. Koumoussi, M. J. Manos, C. Lampropoulos, A. J. Tasiopoulos, W. Wernsdorfer, G. Christou and T. C. Stamatatos, *Inorg. Chem.*, 2010, **49**, 3077; (b) J. P. Fackler and A. Avdeef, *Inorg. Chem.*, 1984, **13**, 1864.
- 16 T. C. Stamatatos, A. Vinslava, K. A. Abboud and G. Christou, *Chem. Commun.*, 2009, 2839.
- 17 S. Nayak, Y. Lan, R. Clérac, C. E. Anson and A. K. Powell, *Chem. Commun.*, 2008, 5698.